Supporting Information

Noble-Metal-Free NiO-MoO_2-CeO_x/N-C Catalysts for Enhanced Catalytic Dehydrogenation of Hydrous Hydrazine

Guizhi Li, Xiaole Shi, Ying Gao, Hongli Wang**

College of Material Science and Engineering, Key Laboratory of Advanced Structural Materials, Ministry of Education, Changchun University of Technology, Changchun, 130012, China

Corresponding Authors' e-mail addresses: gaoying@ccut.edu.cn, wanghongli@ccut.edu.cn

Chemicals: All reagents, including nickel chloride hexahydrate ($NiCl_2 \cdot 6H_2O$), cerium(III) nitrate hexahydrate ($Ce(NO_3)_3 \cdot 6H_2O$), hydrazine monohydrate ($N_2H_4 \cdot H_2O$, HH), sodium borohydride ($NaBH_4$), sulfuric acid (H_2SO_4), anhydrous ethanol (C_2H_5OH), sodium hydroxide (NaOH), 2-methylimidazole ($C_4H_6N_2$), zinc nitrate hexahydrate ($Zn(NO_3)_2 \cdot 6H_2O$), methanol (CH_3OH) and sodium molybdate dihydrate ($Na_2MoO_4 \cdot 2H_2O$) were purchased and used without further purification. Deionized water and ethanol were employed for washing and preparation of reaction solutions.

Synthesis of catalyst: The nitrogen-doped carbon (N-C) framework was synthesized by pyrolyzing ZIF-8 as the precursor. Firstly, 12.06 g of 2-methylimidazole was dissolved in 60 mL of methanol, and this solution was subsequently added into 360 mL of methanol containing 10.92 g of $Zn(NO_3)_2 \cdot 6H_2O$. The mixture was then allowed to react at 30 °C for 24 h. Following this reaction, the resulting ZIF-8 product was

---

*Corresponding authors. E-mail: gaoying@ccut.edu.cn (Y. Gao)
*Corresponding authors. E-mail: wanghongli@ccut.edu.cn (H. Wang)

collected by centrifugation, washed thoroughly with methanol, and finally dried overnight at 70°C. Then the obtained ZIF-8 powder was subjected to a thermal annealing process. Specifically, it was heated to 1000°C for 3 h under an Ar flow at a ramp rate of 5°C min^{-1}, which yielded the initial N-C framework. After this pyrolysis, the framework underwent an acid wash in 0.5 M H_2SO_4 overnight. To complete the stabilization, it was then subjected to a second pyrolysis at 900°C for 1 h under an Ar atmosphere of 5°C min^{-1}.

The NiO-MoO_2-CeO_x/N-C was prepared by a simple wet chemistry route. Typically, for the synthesize of $(NiO)_{0.7}$-$(MoO_2)_{0.3}$-$(CeO_x)_{0.07}$/N-C, 60 mg of N-C was dispersed in 10 mL of deionized water and ultrasonicated for 15 min. Subsequently, an aqueous solution contained $NiCl_2 \cdot 6H_2O$ (0.1 M, 1.4 mL), $Na_2MoO_4 \cdot 2H_2O$ (0.1 M, 0.6 mL) and $Ce(NO_3)_3 \cdot 6H_2O$ (0.1 M, 140 μL) were added to the N-C suspension with magnetic stirring for 1.5 h. Then, the resultant mixture was reduced by adding 40 mg of $NaBH_4$ and stirred at 600 r/min for an additional 30 min. The final product was collected by centrifugation and washed thoroughly with deionized water. For comparison, NiO-MoO_2/N-C, NiO-CeO_x/N-C, NiO/N-C, MoO_2/N-C, and CeO_x/N-C were prepared under identical conditions while keeping the total metal molar amount the same as that used in the ternary NiO-MoO_2-CeO_x/N-C catalyst.

Catalyst characterization: The microstructure and composition of the samples were characterized using field-emission scanning electron microscopy (FESEM, JSM-IT500), transmission electron microscopy (TEM, FEI Talos F200S), and the corresponding energy-dispersive X-ray spectroscopy (EDX). Inductively coupled plasma atomic emission spectroscopy (ICP-AES) was conducted on a Thermo Jarrell Ash (TJA) Atomscan Advantage instrument. Powder X-ray diffraction (XRD) patterns were recorded on a Rigaku RINT-2000 X-ray diffractometer. X-ray photoelectron spectroscopy (XPS) measurements were performed on an ESCALAB MKII spectrometer equipped with an Al Kα X-ray source. Mass spectrometry (MS) analysis of the generated gas was performed using an OmniStar GSD320 mass spectrometer, where Ar was chosen as the carrying gas.

Catalytic performance testing: The as-prepared catalyst was placed in a two-neck flask, with one neck connected to a gas burette and the other to a pressure-equalizing funnel for introducing the $N_2H_4 \cdot H_2O$ (0.5 M, 4 mL) solution. Then, under magnetic stirring (600 r/min), the valve of the pressure-equalizing funnel was opened, and the reaction commenced. During the reaction, the evolved gas was monitored using the gas burette. It is worth noting that before the reaction, all reactants and the catalysts were preheated to the reaction temperature, and no temperature ramp occurred during the reaction. Subsequently, under identical experimental conditions, the catalytic performance of $(NiO)_y$-$(MoO_2)_{1-y}$-$(CeO_x)_{0.07}$/N-C (y = 0.3, 0.5, 0.7, and 0.9; $y = n_{Ni}/（n_{Ni} + n_{Mo})$) catalysts was evaluated. Specifically, the catalytic performance was measured at different temperatures (313 K, 323 K, 333 K, and 343 K) under atmospheric pressure. After the hydrogen generation reaction over the $(NiO)_y$-$(MoO_2)_{1-y}$-$(CeO_x)_{0.07}$/N-C catalyst was completely finished, the suspension was centrifuged. Then, under magnetic stirring, fresh $N_2H_4 \cdot H_2O$ aqueous solution (0.5 M, 4 mL) was again added to the reaction flask. Subsequently, the released gas was monitored by the gas burette. Finally, the recycling experiment of the as-synthesized catalyst was repeated four times at 313 K under atmospheric pressure.

Furthermore, to investigate the influence of concentration on catalytic dehydrogenation, two sets of experiments were performed. For the HH concentration study, the as-prepared catalyst was placed in a two-neck flask connected to a gas burette and a pressure-equalizing funnel. Different concentrations of $N_2H_4 \cdot H_2O$ solution (0.3, 0.4, 0.5, and 0.6 M, 4 mL) were introduced separately under magnetic stirring (600 r/min), and the evolved gas was monitored. For the catalyst concentration study, a fixed volume $N_2H_4 \cdot H_2O$ solution was used, while the amount of catalyst was varied to achieve catalyst concentrations of (0.125, 0.100, 0.075, and 0.050 M, 2 mL).

To investigate the influence of alkalinity, 4 mL of 0.5 M $N_2H_4 \cdot H_2O$ solution containing different amounts of NaOH (2.4, 4.8, 7.2, 9.6 mmol) was placed in a pressure-equalizing funnel. The corresponding pH values of these solutions were 13.78, 14.08, 14.26, and 14.38, respectively. The catalyst was placed in a two-neck flask. Under magnetic stirring, the NaOH-containing hydrazine solution was then added dropwise from the funnel to start the reaction. The evolved gas was monitored using a gas burette.

Calculation methods: The turnover frequency (TOF, mol H_2 mol cat.$^{-1}$ h^{-1}) was calculated according to Eq. (1):

$$\mathrm{TOF}=\frac{P_{\mathrm{atm}}V_{\mathrm{H_2}}/\mathrm{R}T}{n_{\mathrm{catalyst}}t} \tag{1}$$

where T is the corresponding temperature, V_{H2} is the volume of hydrogen generated at 100% conversion for the overall TOF (or at 20% conversion for the initial TOF), t is the time required to reach the corresponding conversion, P_{atm} is the standard atmospheric pressure, $n_{catalyst}$ is the amount of catalyst (in mmol), and R is the universal gas constant (8.314 J mol^{-1} K^{-1}).

The relationship between TOF and temperature followed the Arrhenius behavior, expressed by Eq. (2):

$$\mathrm{lnTOF} = \mathrm{lnA} - E_a/\mathrm{R}T \qquad (2)$$

where A is the pre-exponential factor and E_a represents the apparent activation energy.

Supplementary Figures

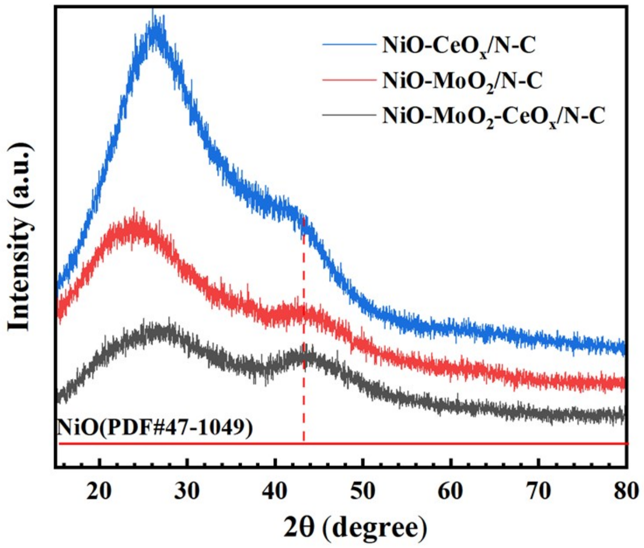

Fig. S1 XRD spectra of NiO-MoO_2-CeO_x/N-C, NiO-MoO_2/N-C, and NiO-CeO_x/N-C.

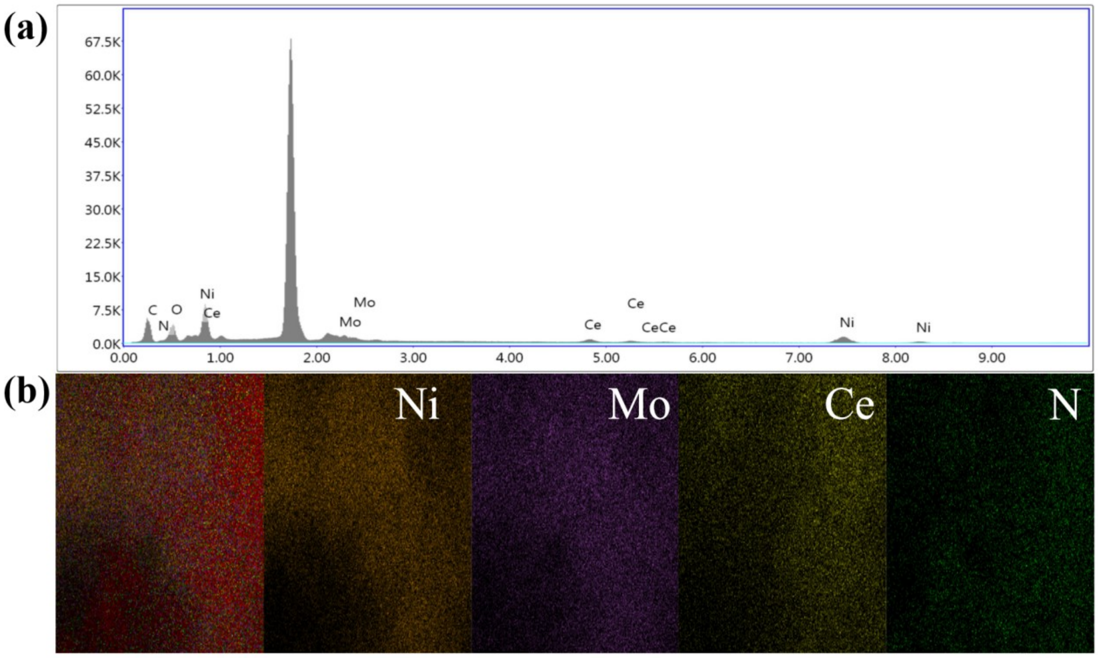

Fig. S2 (a) EDX spectrum, (b) SEM elemental mapping images of NiO-MoO_2-CeO_x/N-C.

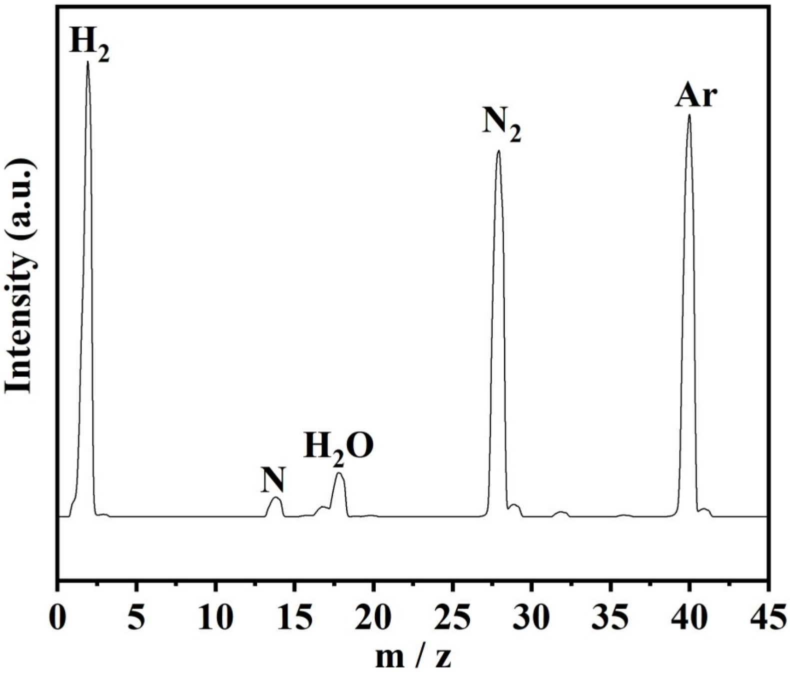

Fig. S3 Mass spectrum of the evolved gas during catalytic dehydrogenation of hydrous hydrazine.

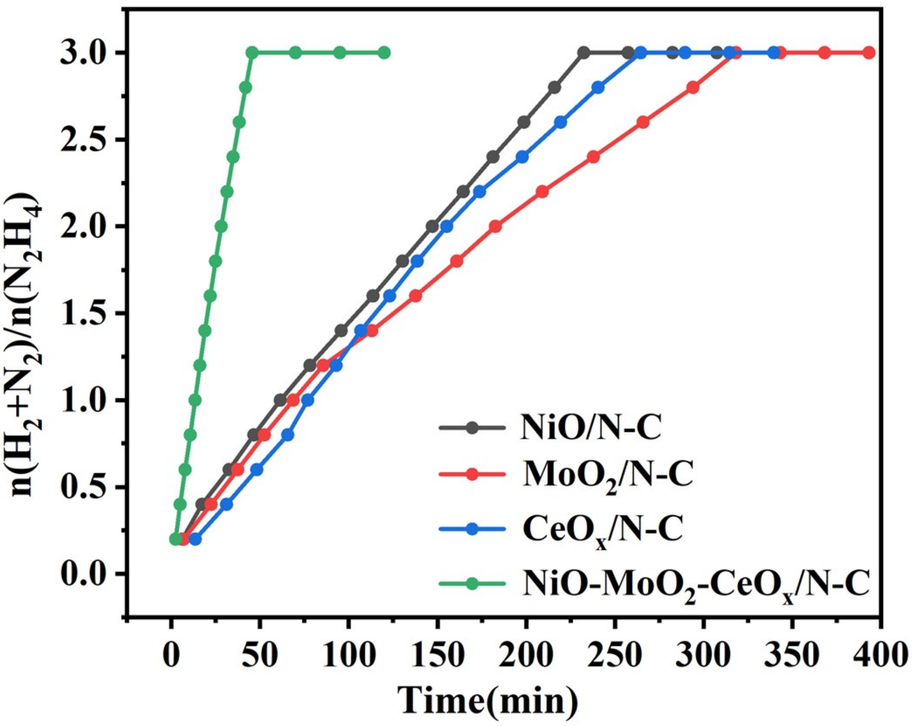

Fig. S4 Hydrogen generation as a function of reaction time for HH dehydrogenation over NiO/N-C, MoO_2/N-C, CeO_x/N-C, and NiO-MoO_2-CeO_x/N-C catalysts at 313 K.

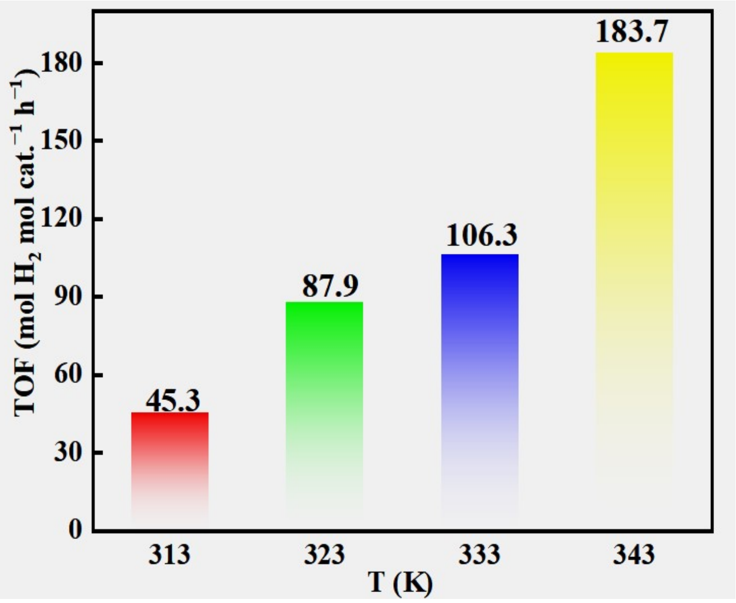

Fig. S5 TOF values for HH dehydrogenation catalyzed by NiO-MoO_2-CeO_x/N-C at different temperatures.

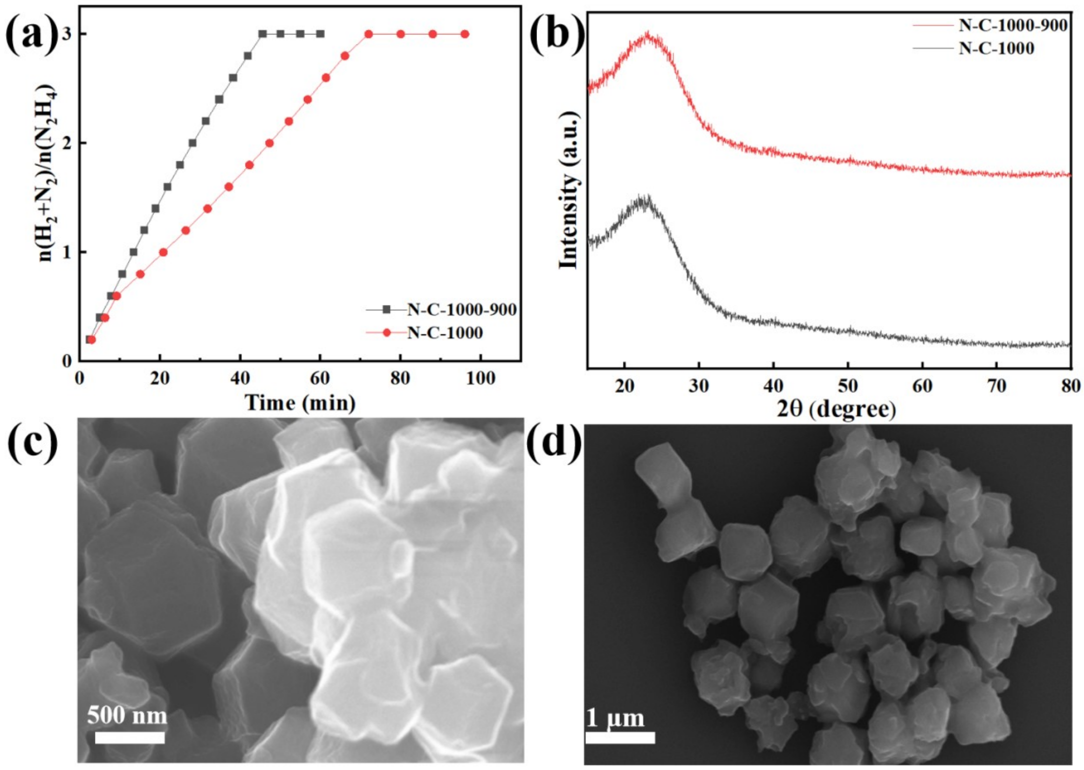

Fig. S6 (a) Hydrogen generation versus time for HH dehydrogenation catalyzed by NiO-MoO$_2$-CeO$_x$ supported on N-C prepared under different calcination conditions, (b) XRD patterns of N-C-1000 and N-C-1000-900, SEM images of (c) N-C-1000 and (d) N-C-1000-900.

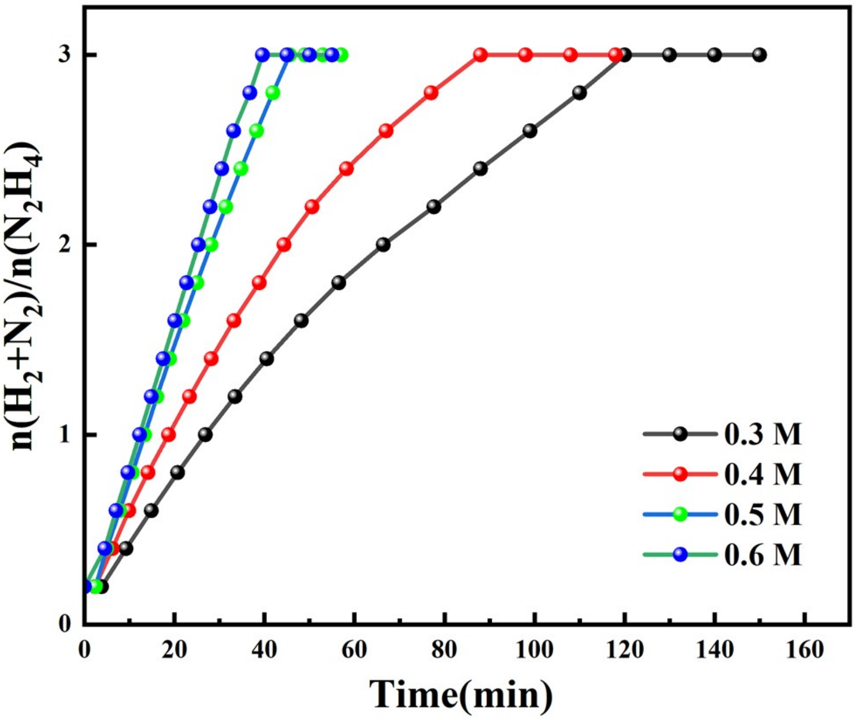

Fig. S7 The relationship between the H_2 generation rate and varying HH concentration (0.3 M, 0.4 M, 0.5 M, and 0.6 M, 4 mL) at a fixed concentration of NiO-MoO$_2$-CeO$_x$/N-C.

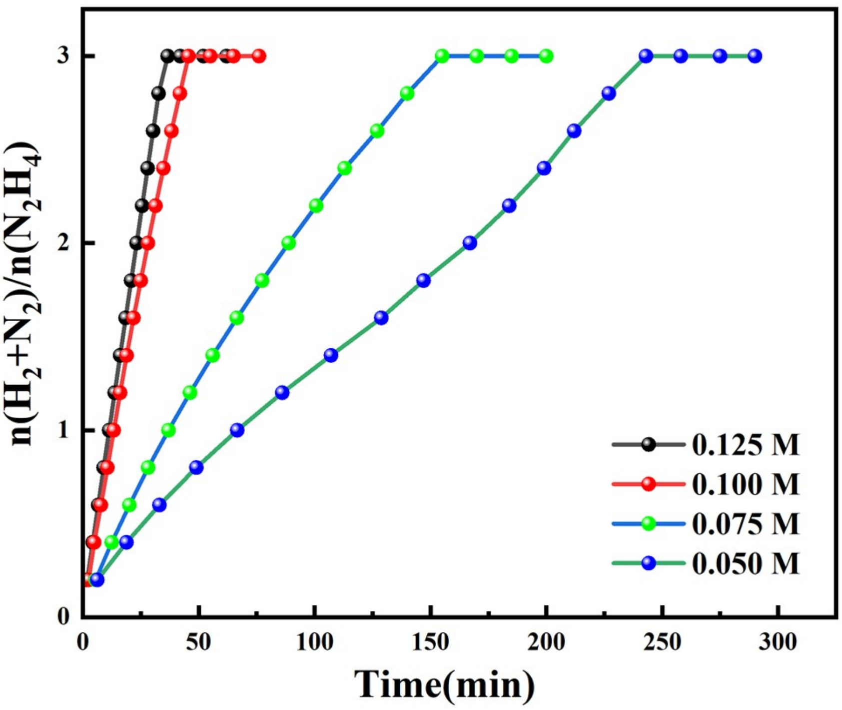

Fig. S8 Stoichiometric H_2 evolution in aqueous solution containing a fixed amount of HH at various catalyst concentrations (0.125, 0.100, 0.075, and 0.050 M, 2 mL).

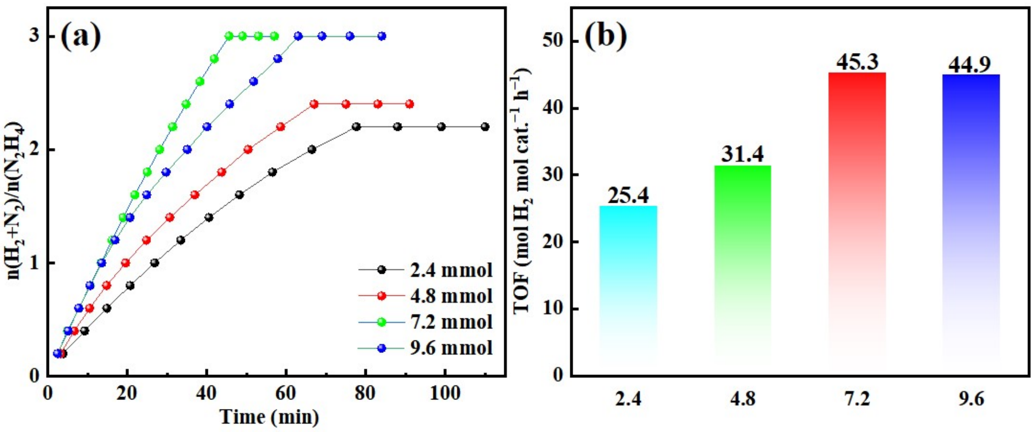

Fig. S9 (a) Effect of different NaOH amounts on the catalytic performance of NiO-MoO$_2$-CeO$_x$/N-C in hydrogen generation from HH dehydrogenation at 313 K (n_{CeO_x} = 7.0%, n_{Ni}/n_{Mo} = 7:3, $n_{N_2H_4}$ = 2 mmol) and (b) the corresponding TOF values.

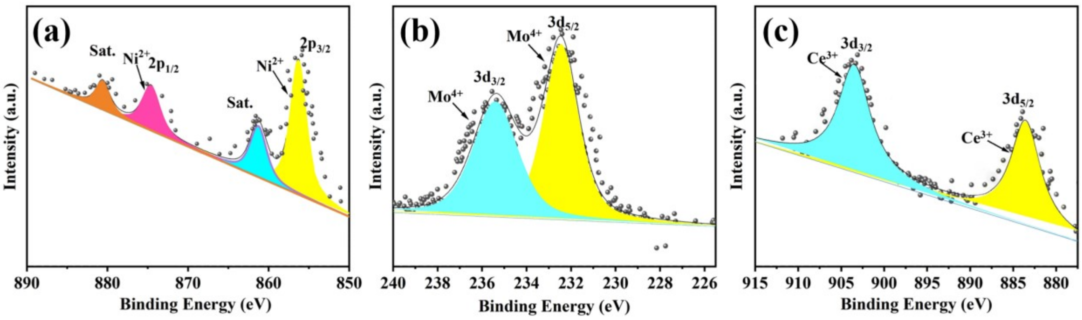

Fig. S10 High-resolution XPS spectra of (a) Ni 2p, (b) Mo 3d, and (c) Ce 3d for the NiO-MoO_2-CeO_x/N-C catalyst after cycling durability tests.

Supplementary Table

Table S1 The Ni, Mo, and Ce contents and the corresponding Ni/Mo/Ce molar ratios of NiO-MoO_2-CeO_x/N-C before and after cyclic tests obtained by ICP.

Sample	ICP results			
	Ni loading (mg)	Mo loading (mg)	Ce loading (mg)	Ni: Mo: Ce (at. %)
NiO-MoO_2-CeO_x/N-C before cyclic tests	5.23	3.67	1.25	65.4: 28.1: 6.5
NiO-MoO_2-CeO_x/N-C after cyclic tests	4.89	3.43	1.17	65.1: 28.2: 6.7

Table S2 TOF and E_a values for different catalysts in hydrogen production from HH decomposition.

Catalyst	**TOF (mol H_2 mol cat.$^{-1}$ h^{-1})**	**T (K)**	**E_a (kJ/mol)**	**Ref.**
$NiO-MoO_2-CeO_x/N-C$	**45.3**	**313**	**39.2**	**This work**
$Ni_9Mo_1(Pr_2O_3)_{0.375}$	62	343	43.2	[17]
$Ni_3Cr/NiO-CrO_x$	39.8	323	53.1	[36]
$Ni_{91}Ir_9/CeO_2$	-	323	50.8	[37]
NiMo/Ni-Mo-O	54.5	323	55	[38]
NiFe/Cu	17.6	343	47	[39]
$Ni_4W/WO_2/NiWO_4$	33	323	-	[40]
$NiPt_{0.057}/Al_2O_3$	16.5	303	52.5	[41]
$Ni_{0.6}Fe_{0.4}Mo$	28.8	323	50.7	[42]
$Ni_{30}Fe_{30}Pd_{40}$	21.4	318	40	[43]
$Ni_{0.9}Pt_{0.1}/Ce_2O_3$	28.1	298	42.3	[44]
$Ni/NH_2-MIL-125$	108.1	323	59.9	[45]
$Ni/TiO_2-NH_2-MIL-101$	422	343	50.9	[46]